

Simulating the collapse transition of a two-dimensional semiflexible lattice polymer

Jie Zhou, Zhong-Can Ou-Yang, and Haijun Zhou

Institute of Theoretical Physics, the Chinese Academy of Sciences, Beijing 100080, China

It has been revealed by mean-field theories and computer simulations that the nature of the collapse transition of a polymer is influenced by its bending stiffness ϵ_b . In two dimensions, a recent analytical work demonstrated that the collapse transition of a partially directed lattice polymer is always first-order as long as ϵ_b is positive [H. Zhou *et al.*, Phys. Rev. Lett. **97**, 158302 (2006)]. Here we employ Monte Carlo simulation to investigate systematically the effect of bending stiffness on the static properties of a 2D lattice polymer. The system's phase-diagram at zero force is obtained. Depending on ϵ_b and the temperature T , the polymer can be in one of three phases: crystal, disordered globule, or swollen coil. The crystal-globule transition is discontinuous, the globule-coil transition is continuous. At moderate or high values of ϵ_b the intermediate globular phase disappears and the polymer has only a discontinuous crystal-coil transition. When an external force is applied, the force-induced collapse transition will either be continuous or discontinuous, depending on whether the polymer is originally in the globular or the crystal phase at zero force. The simulation results also demonstrate an interesting scaling behavior of the polymer at the force-induced globule-coil transition.

PACS numbers: 82.35.Lr, 61.41.+e, 64.60.Cn

Keywords: collapse transition, semiflexible polymer, self-avoiding, Monte Carlo simulation, scaling behavior, bending stiffness

I. INTRODUCTION

A polymer is a linear chain of monomers¹. The configuration of a long polymer in solution is influenced by three different types of interactions. Firstly, there are complicated interactions between monomers such as hydrogen-bonding, weak van der Waals attraction, and electrostatic interactions. Monomer-monomer interactions can also be mediated by solvent molecules, e.g., the attraction between two negatively charged monomers due to the mediation of a multi-valent positive charge (Mg^{2+} , for example). In theoretical models of homologous polymers, the monomer-monomer interactions can be represented by a potential energy $U(\mathbf{r}_i, \mathbf{r}_j)$ between two monomers at position \mathbf{r}_i and position \mathbf{r}_j . Monomer-monomer interactions can be either attractive or repulsive. If the total interaction between a pair of monomers is attractive, it tends to bring different parts of the polymer together. At low temperatures, these monomer-monomer attractive interactions result in the formation of compacted (globular) polymer configurations. The volume of the polymer shrinks as much as possible to minimize the total monomer-monomer contacting energy. In such a globular configuration, the radius of gyration R_g of the polymer scales with the polymer length N as $R_g \propto N^{1/d}$, with d being the spatial dimension². (For polymers in solution, $d = 3$; for polymers attached on the membrane of mobile lipids³, $d = 2$).

In the solution, solvent molecules collide frequently with the polymer due to thermal agitation. These collisions tend to make the polymer to take disordered and swollen coil configurations. At high temperatures, thermal effects win over monomer-monomer attractions. Consequently the polymer will take a randomly coiled shape, whose radius of gyration scales with the polymer length N as $R_g \propto N^\nu$, where the scaling exponent $\nu \approx 3/(d+2)$ according to the Flory mean-field theory^{2,4,5} and 2D exact calculations⁶.

Between the above-mentioned low-temperature globular phase and high-temperature swollen coil phase, there exists also another critical phase when the temperature is at a critical point T_θ , the so-called theta-point¹. At T_θ , the polymer achieves a delicate balance among monomer-monomer attractions, excluded-volume repulsions, and configurational entropy. The polymer's gyration radius follow another new scaling law $R_g \propto N^{\nu_{cr}}$, with the critical exponent $\nu_{cr} = 4/7$ for 2D polymers^{5,7} and $\nu_{cr} = 1/2$ for 3D polymers^{2,4}.

The third type of interactions are external forces. In recent single-molecule manipulation experiments, external forces on the order of piconewtons (10^{-12} N) can be applied on the ends of a polymer such as DNA⁸. When the external force field is sufficiently weak, the configuration of a self-attracting polymer is not affected by the force, since the attractive interaction between monomers is stronger to keep itself remain compacted. On the other hand, when the external force is sufficiently large, the polymer will be elongated considerably along the force direction, and the end-to-end distance of the polymer chain scales *linearly* with polymer length N .

The overall shape of a self-attracting polymer can be dramatically changed by changing environmental temperature and/or external force. The globule-coil structural transition is a fundamental issue in polymer physics. The nature of this transition has been studied extensively in the past several decades by experimental, theoretical, and simulation approaches^{1,2,5,9,10,11,12,13,14,15,16,17,18,19}. Certain degree of consensus has been achieved on various aspects of the poly-

mer globule-coil transition, but there are still some unresolved important issues. For a flexible self-attractive polymer, mean-field theories predicted a second-order continuous globule-coil phase-transition as the ambient temperature is elevated. This prediction was confirmed by more recent analytical calculations^{20,21,22} in 2D; however, there are still some controversies in the literature concerning Monte Carlo simulations in 3D (for example, Refs. [23,24] believed that the 3D globule-coil transition is a first-order phase-transition in the thermodynamic limit). The force-induced globule-coil transition is found to be first-order in 3D and to be second-order in 2D^{20,25}.

The phase behavior of a semiflexible polymer is even more complex. For a semiflexible polymer at very low temperature, the arrangement of its segments in a globular conformation may be highly ordered. This is driven by the desire of minimizing the total bending energy. The polymer are therefore in a compact crystal phase. As temperature increases, this crystalline order may be destroyed so as to gain configurational entropy, but the polymer is still in a (disordered) globular form. This crystal-globule transition is predicted to be a first-order phase-transition both by exactly solvable models^{9,10} and by 3D mean-field theory and Monte-Carlo simulation studies^{13,14,26}. When the temperature is further increased to the θ temperature, the polymer globular conformation will change again to a swollen coil conformation. This globule-coil transition is believed to be second-order^{2,13,14,23,27,28}. The θ temperature appears to be insensitive to the polymer's bending stiffness^{13,14,29}. However, if the bending stiffness of the polymer is sufficiently large, the solid-globule and globule-coil transitions may occur at the same temperature, resulting in a single first-order solid-coil structural transition¹³.

The force-induced collapse-transition have also been studied in recent years. For 3D polymers, the transition is shown to be first-order no matter whether the polymer is flexible or semiflexible^{21,25}. For 2D flexible polymer, this transition is believed to be second-order^{20,25,30}; while the results of an exactly solvable model²² suggest that the order will change to be first-order when the polymer is semiflexible.

In this work, through a series of Monte Carlo simulations we aim at a comprehensive understanding of the phase behavior of a 2D semiflexible polymer under the action of temperature and external force. We pay special attention on the effect of bending stiffness. First we obtain the phase-diagram of the polymer at zero force using temperature T and bending stiffness ϵ_b as two control parameters. At low ϵ_b , the polymer can reside in three phases: crystal, disordered globule, and swollen coil. The crystal-globule transition is first-order and the globule-coil transition is second-order. When ϵ_b exceeds some threshold value, however, the intermediate globular phase of the polymer disappears. The polymer then has only one crystal-coil transition, which is first-order. After the zero-force phase-diagram of the polymer is known, we continue to study its stretching behavior. We find that if at zero-force the polymer is in the crystal phase, the applied force will cause a first-order crystal-coil transition. But if the polymer is originally in the disordered globule phase, the force-induced collapse transition will be continuous. In the later case, the critical scaling behavior of the extension of the polymer with chain length at the transition point is obtained by MC simulation. To predict this critical scaling behavior analytically requires further work. With these results, the present simulation work enriches our understanding of the structural properties of 2D self-attractive polymers. It contributes to a full characterization of semiflexible polymers both in 3D and on a surface.

The paper is organized as follows: The next section introduces the model system; and the Monte Carlo simulation method is described in Sec. III. Section IV and Sec. V focus, respectively, on temperature- and force-induced structural transitions. We conclude this work in Sec. VI.

II. THE MODEL

We study by MC simulations the phase behaviors of a 2D self-avoiding lattice polymer. The polymer is on a square lattice with edge length a . The bond length between two consecutive monomers i and $i+1$ of the polymer also equals to a . One end of the polymer is fixed; the other end is free (without external force) or is being stretched by an external force f along the x -axis of the surface (see Fig. 1).

If two monomers i and j of the polymer (with $|j-i| \geq 2$) occupy nearest-neighboring sites on the square lattice, there is an attractive energy of magnitude ϵ . If in a configuration \mathcal{C} there are a total number of N_c such contacts, then the total contacting energy is $-N_c\epsilon$. For semiflexible polymers, there are also bending energies. In the lattice polymer, whenever the configuration \mathcal{C} makes a turn (with three consecutive monomers not staying on a rectilinear line) there is an energy penalty ϵ_b . Denote the total number of turns in the configuration \mathcal{C} as N_b , the total bending energy is then $N_b\epsilon_b$. The energy contributed by the external force is equal to $-fx$, where x is the x -axis component of the end-to-end distance vector of the polymer. For a given configuration \mathcal{C} , the total configurational energy is expressed as

$$E(\mathcal{C}) = -N_c\epsilon + N_b\epsilon_b - fx . \quad (1)$$

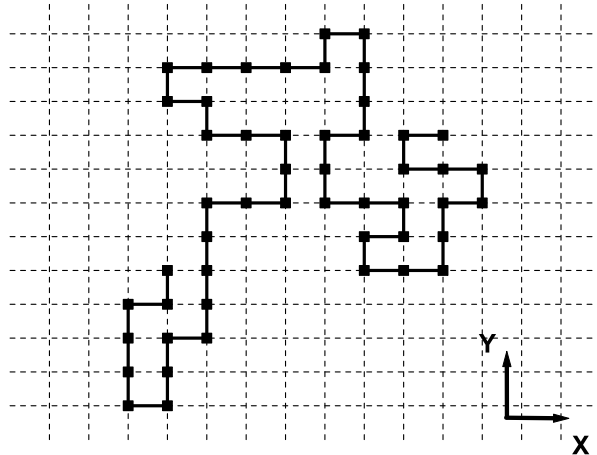


FIG. 1: A polymer on a 2D square lattice with lattice constant a . The configuration of the polymer fluctuates over time under the joint action of monomer-monomer contacting interactions, bending energy, external force, and thermal energy.

The partition function of the polymer is

$$Z = \sum_{\mathcal{C}} \exp\left(-\frac{E(\mathcal{C})}{k_B T}\right), \quad (2)$$

where k_B is the Boltzmann constant and T is the environmental temperature.

In the following MC simulations, energy unit is set to be ϵ , length unit is set to be a , k_B is set to be unity, and force unit is set to be ϵ/a . In the absence of external force, the 3D version of this lattice-polymer was previously studied by mean-field theory and by MC simulations in Ref. [13].

III. MONTE CARLO SIMULATION METHOD

Many different Monte Carlo procedures are documented in the literature (see, e.g., Refs. [24,31,32,33,34,35,36]) to sample configurations of a polymer according to the Boltzmann distribution

$$p(\mathcal{C}) = \frac{\exp(-E(\mathcal{C})/(k_B T))}{Z} \quad (3)$$

where Z is the total partition function of the polymer as given by Eq. (2). The present MC procedure, which is based on the idea of importance sampling (see, e.g., textbook [37]), is inspired mainly by the earlier work of Refs. [14,31,32,33]. In sampling polymer configurations, the transition probability $T(\mu \rightarrow \nu)$ for the polymer to evolve from an old configuration μ to a new configuration ν is given by³⁷:

$$T(\mu \rightarrow \nu) = g(\mu \rightarrow \nu) \times A(\mu \rightarrow \nu). \quad (4)$$

In this equation, $g(\mu \rightarrow \nu)$ is the probability of proposing a particular updated configuration ν from the old configuration μ , and $A(\mu \rightarrow \nu)$ is the probability of accepting this updates. To ensure detailed balance, $A(\mu \rightarrow \nu)$ is chosen such that

$$A(\mu \rightarrow \nu) = \begin{cases} \eta(\mu \rightarrow \nu)e^{-\beta(E_\nu - E_\mu)}, & \text{if } \eta(\mu \rightarrow \nu)e^{-\beta(E_\nu - E_\mu)} < 1 \\ 1, & \text{if } \eta(\mu \rightarrow \nu)e^{-\beta(E_\nu - E_\mu)} \geq 1 \end{cases} \quad (5)$$

where $\eta(\mu \rightarrow \nu) \equiv g(\nu \rightarrow \mu)/g(\mu \rightarrow \nu)$.

In this paper, we use six different types of elementary updating rules for the polymer's configuration (Fig. 2). These updating rules are described in some detail here.

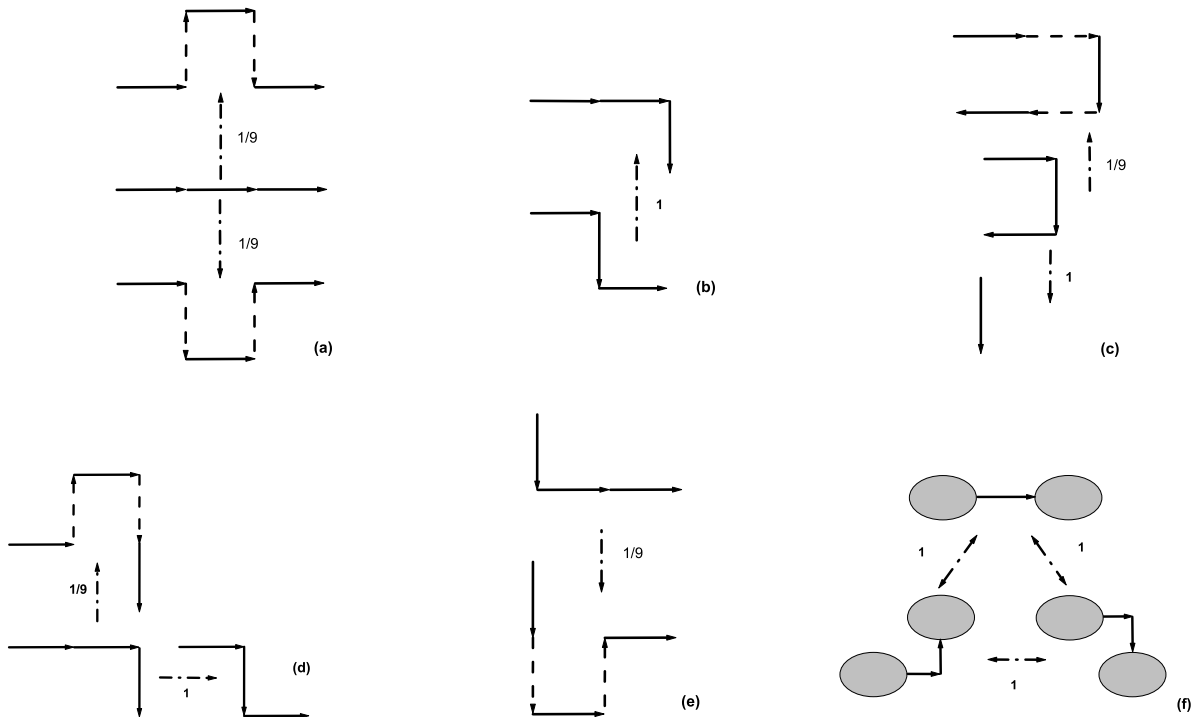


FIG. 2: Six different types of elementary configurational updates of the present MC simulation method.

- rule-1 Bonds $i - 1$, i , and $i + 1$ are parallel to each other [Fig. 2(a)]. After the update, a hairpin is formed right after bond $i - 1$, with bond $i + 1$ being at the head of the hairpin. The polymer segment from bond $i + 3$ to bond N reptates along its old contour and the free end of the polymer shrinks by two bonds.
- rule-2 Bond i is perpendicular to bonds $i - 1$ and $i + 1$ [Fig. 2(b)]. After the update, i becomes parallel to bond $i - 1$, while bond $i + 1$ is perpendicular to both bond $i - 1$ and bond i .
- rule-3 Bonds $i - 1$, i , and $i + 1$ forms a hairpin, with bond i being at the head [Fig. 2(c)]. After the update, with probability one-half, the stem length of this hairpin increases or decreases by one bond length. This stem length change is achieved by reptation, with the free end of the polymer draws back or stretches out by two bonds. If the free end of the polymer stretches out, the orientations of the last two bonds are randomly and independently assigned.
- rule-4 Bond $i + 1$ is perpendicular to both bonds $i - 1$ and i [Fig. 2(d)]. With probability one-half, after the update bond i becomes perpendicular to both bonds $i - 1$ and $i + 1$. With the remaining probability one-half, after the update bond $i + 1$ becomes the head of a hairpin while the polymer segment from bond $i + 3$ to bond N reptates along its old contour, and the free end of the polymer shrinks by two bonds.
- rule-5 Bond $i - 1$ is perpendicular to both bonds i and $i + 1$ [Fig. 2(e)]. After the update, bond $i + 1$ becomes the head of a hairpin, while the polymer segment from bond $i + 3$ to N reptates along its old contour and the free end of the polymer shrinks by two bonds.
- rule-6 The polymer segment from bond $i + 1$ to bond N is rotated as a whole with respect to bond i clockwise or counter-clockwise by an angle of $\pi/2$ or π [Fig. 2(f)]. This elementary update causes a large change in the chain's configuration.

We have taken special care to ensure that during these MC updating processes, (1) no two monomers occupy the same site, (2) detailed balance is not violated. To ensure detailed balance, the ratios $\eta(\mu \rightarrow \nu)$ of Eq. (5) are carefully determined and given in Fig. 2. (When the chosen bonds of Fig. 2 are located at the ends of the polymer, the $\eta(\mu \rightarrow \nu)$ values will be different from the values shown in the figure.) With the present MC procedure, we are able to simulate polymer lengths up to $N = 3,000$, which is much longer than the lengths of several hundreds used in some previous MC simulations^{14,27,33}.

IV. TEMPERATURE-INDUCED COLLAPSE TRANSITIONS

We begin with the temperature-induced collapse transitions at zero external force ($f \equiv 0$). We will obtain numerically the phase diagram of the polymer in the plane spanned by temperature T and bending stiffness ϵ_b .

A. Flexible polymers ($\epsilon_b = 0$)

First we focus on flexible chains. The equilibrium properties of a flexible lattice polymer are well-known, therefore this system can be used to check the validity of our MC simulation method. Let us denote by R_N the end-to-end distance of the polymer of N bonds. (In our simulations, we use R_N instead of the gyration radius to characterize the structural properties of a polymer. R_N behaves in the same way as the gyration radius³⁸ and it can be computed with less statistical variance²⁷). As mentioned in Sec. I, there is the following scaling relationship between R_N and the polymer size N :

$$\langle R_N^2 \rangle \sim N^{2\nu}, \quad (6)$$

where $\langle \dots \rangle$ means thermal average. At low temperatures, the polymer is in the compacted globular form, and the scaling exponent ν approaches $1/2$ in $2D^{4,39,40}$; at high temperatures, the configuration of the polymer is reminiscent of a self-avoiding random walk, and ν approaches the other limiting value of $3/4$ [6]. At the globule-coil phase transition temperature T_θ , the polymer is in a critical state, and the scaling exponent ν takes yet another value $\nu = \nu_{cr} = 4/7$ [7]. The scaling exponent ν of Eq. (6) in general may have a weak dependence on the polymer length $N^{2,41,42,43,44,45}$. However, at the critical θ state, ν will be independent of N . If we plot $\langle R_N^2 \rangle / N^{8/7}$, then curves for different lengths N should intersect at the θ temperature.

Figure 3 shows the relationship between $\langle R_N^2 \rangle / N^{8/7}$ and temperature for chains of different lengths N . Different curves indeed intersect at the same point when $T = T_\theta \approx 1.50$. Therefore, the present MC method is able to correctly predict the critical exponent of $\nu_{cr} = 4/7$ for a 2D flexible polymer. The predicted T_θ value is also in agreement with the value of $T_\theta = 1.54 \pm 0.05$ as given by Ref. [46].

When there is no external force, the specific heat $c(T)$ of the system as a function of T can be obtained through $c(T) = \beta^2 (\langle E^2 \rangle - \langle E \rangle^2) / N$ and is shown in Fig. 4. As the chain length N increases, surface effect (which reduces the total number of contacts) of the globular phase becomes less important, therefore the temperature T_p at which $c(T)$ reaches maximum increases with N . The MC simulation data suggest that T_p approaches the critical temperature T_θ according to the following formula $T_p = T_\theta [1 - (c_0/N)^s]$ with $c_0 = 3.0 \pm 1.0$ and $s = 0.44 \pm 0.04$. The peak value $c(T_p)$

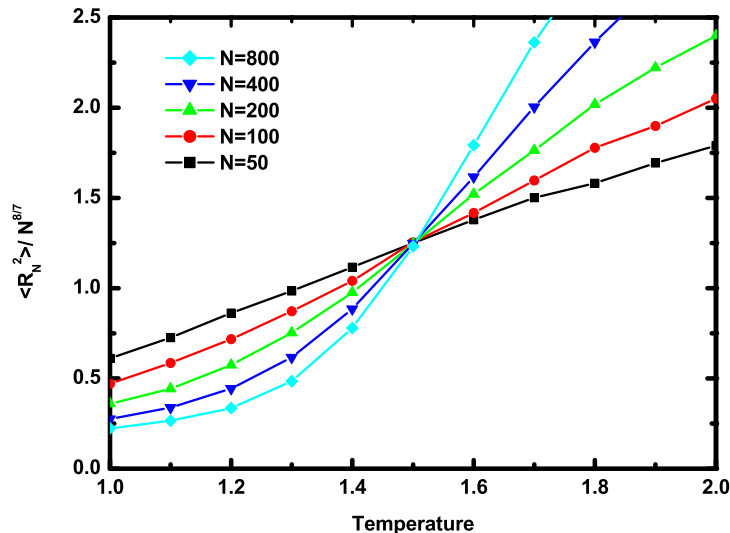


FIG. 3: (Color Online) The relationship between $\langle R_N^2 \rangle / N^{8/7}$ and temperature T for a flexible lattice polymer of different lengths N . Different curves intersect at the θ temperature of $T_\theta \approx 1.50$.

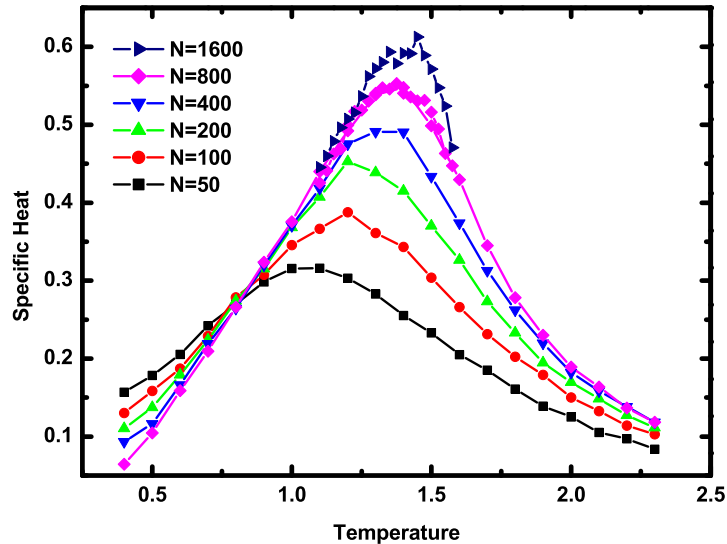


FIG. 4: (Color Online) The specific heat $c(T)$ for a 2D flexible lattice polymer of different lengths N .

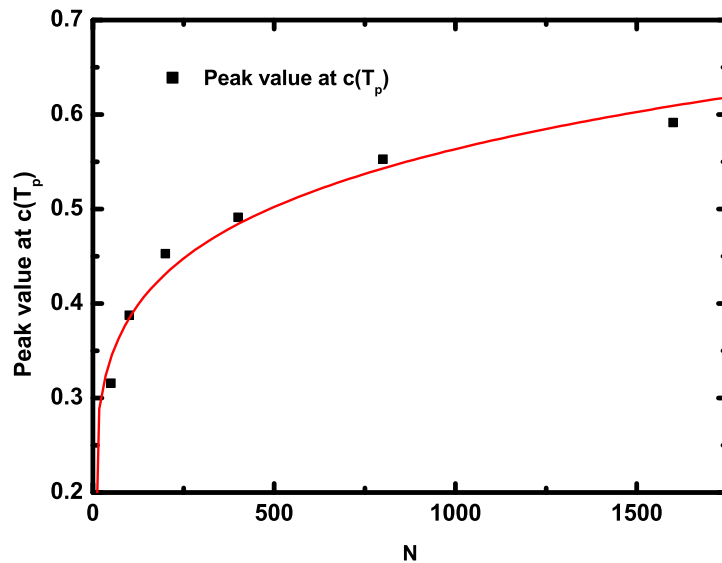


FIG. 5: The relation between the peak values $c(T_p)$ of the specific heat and chain length for a flexible polymer ($\epsilon_b = 0$). The solid line is the fitting curve $c(T_p) = bN^\alpha$ with $b = 0.179 \pm 0.017$ and $\alpha = 0.166 \pm 0.015$.

of the specific heat diverges with chain length N according to $c(T_p) \propto N^\alpha$ with $\alpha = 0.166 \pm 0.015$ (see Fig. 5). From this finite-size scaling behavior we estimate the crossover exponent⁴⁷ $\phi \equiv 1/(2 - \alpha)$ to be $\phi \approx 0.545$. This value is in agreement with the value of $\phi = 0.52 \pm 0.07$ given by Ref. [46].

Taking together, the simulation results of this subsection, in confirmation to various earlier efforts, predict a continuous globule-coil phase-transition for a self-attracting flexible 2D polymer.

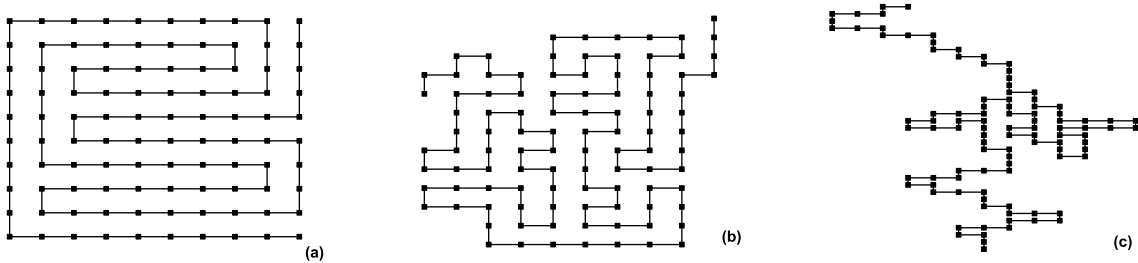


FIG. 6: Typical configurations of a semiflexible polymer in the crystal (a), disordered globule (b), and extended random coil (c) phase.

B. Semiflexible polymers

When bending stiffness ϵ_b of the polymer is positive, the polymer's configuration is also influenced by bending energies. At very low temperatures entropic effect is not important, then the polymer will favor those compact configurations which have the maximal number of monomer-monomer contacts and the minimal number of bends. These are highly ordered crystal configurations as illustrated in Fig. 6(a). In such a crystal configuration^{9,10,48} long segments of the polymer stack onto each other, and the total number of bends N_b scales only sub-linearly with chain length N . Let us define two order parameters n_b (the density of bends) and n_c (the density of contacts) as

$$n_b = \frac{N_b}{N}, \quad (7)$$

$$n_c = \frac{N_c}{N}. \quad (8)$$

For a polymer in a crystal conformation, we have $\lim_{N \rightarrow \infty} n_b = 0$ and $\lim_{N \rightarrow \infty} n_c$ of order unity. The overall shape of a polymer crystal may be a rectangle rather than a square, the aspect ratio of which depending on ϵ_b . When

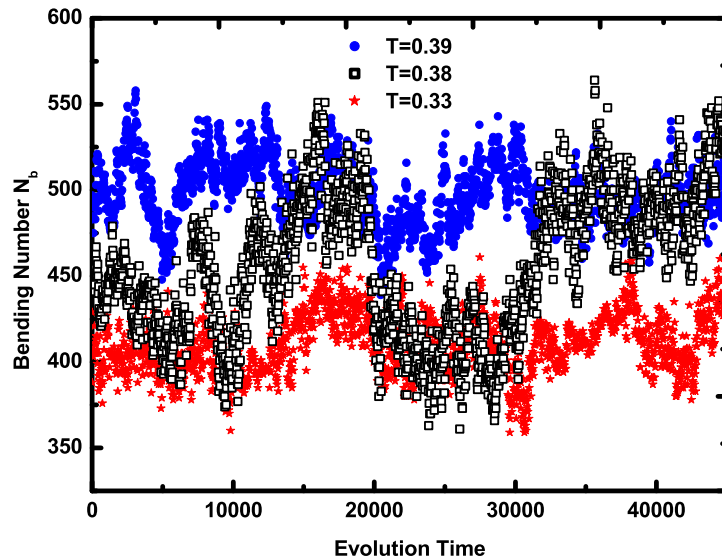


FIG. 7: (Color Online) Evolution of the configuration of a semiflexible polymer with bending stiffness $\epsilon_b = 0.3$ and length $N = 2,000$. The vertical axis is the number of bends N_b in the configuration, and the horizontal axis is the evolution time in terms of MC steps. (At time zero of the figure the system has already reached equilibrium.) The temperature is $T = 0.33$ (red stars), 0.38 (black open squares), and 0.39 (green filled squares).

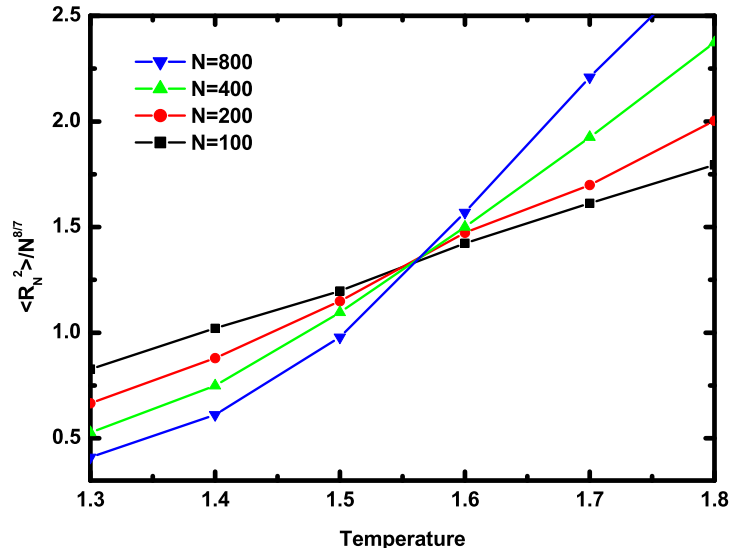


FIG. 8: (Color Online) The relationship between $\langle R_N^2 \rangle / N^{8/7}$ and temperature T for a semiflexible polymer of different lengths N . The bending stiffness is $\epsilon_b = 0.6$. Different curves intersect at the θ temperature of $T_\theta \approx 1.55$.

temperature is elevated, the entropy effect becomes more and more important. At certain point the crystal order of the polymer will be destroyed. For ϵ_b being small, when crystal order disappears the monomer-monomer contacting interactions may still be very significant. Then the polymer will take disordered globular shapes (Fig. 6(b)). In a disordered globular configuration, both the order parameters n_b and n_c are of order unity. When temperature is further increased, the globular configuration will again become unstable, and the polymer will transit to the phase of swollen random coil (Fig. 6(c)).

The crystal-globule structural transition is a first-order phase-transition in the thermodynamic limit of $N \rightarrow \infty$, similar to the solid-liquid transition of water at 0°C . This is demonstrated in Fig. 7 for the evolution of the total bending number N_b of a polymer with length $N = 2,000$ and bending stiffness $\epsilon_b = 0.3$. At temperature $T = 0.33$, N_b fluctuates around $N_b^{(1)} \approx 410$. At $T = 0.39$, N_b fluctuates around the value of $N_b^{(2)} \approx 510$. While at the intermediate temperature $T = 0.38$, N_b jumps between these two values $N_b^{(1)}$ and $N_b^{(2)}$, indicating that the system is bistable. On the other hand, at each of these temperatures, the histogram of the number of contacts N_c has only one peak. The crystal-globule transition temperature increases with the bending stiffness ϵ_b of the polymer.

When the temperature is further increased to $T \approx 1.5$, a second structural transition takes place. This globule-coil transition is second-order, as can be inferred from Fig. 8. This figure shows the value of $\langle R_N^2 \rangle / N^{8/7}$ as a function of temperature for a semiflexible polymer of bending stiffness $\epsilon_b = 0.6$ and different lengths N (similar results were obtained for $\epsilon_b = 0.3$ and $\epsilon_b = 1.0$). Figure 8 is qualitatively the same as Fig. 3 of a flexible polymer. The only quantitative difference is that the transition θ temperature is slightly increased. At the globule-coil transition point, the scaling exponent ν_{cr} of the semiflexible polymer is the same as that of a flexible polymer. Therefore, bending stiffness does not influence the scaling behavior of a polymer in its critical θ state. The globule-coil transition temperature is also not very sensitive to the bending stiffness.

In the crystal or the disordered globular phase, the size of the lattice polymer scales with chain length in a square-root law, i.e., $R_N^2 = c_1 N$ with $c_1 \approx 0.6$. The value of the prefactor c_1 has no obvious change at the crystal-globule transition temperature; it is also insensitive to the bending stiffness ϵ_b . When the temperature approaches or goes beyond the globule-coil transition temperature T_θ , however, c_1 increases quickly with T (because the square-root scaling law no-longer holds).

When the bending stiffness of the semiflexible polymer exceeds a threshold value of $\epsilon_b \approx 1.5$, the intermediate disordered globule phase disappears. The polymer will exist only in two phases, either the low-temperature crystal phase or the high-temperature swollen coil phase, and the structural transition between these two phases is first-order. For a semiflexible polymer with $\epsilon_b = 5$ and length N , Fig. 9 shows the relationship between the density of contacts n_c and temperature T . As N becomes sufficiently large (e.g., $N = 1,600$) we notice a dramatic drop of n_c at $T \approx 3.0$, indicating the existence of a globule-coil transition. For T close to this transition temperature,

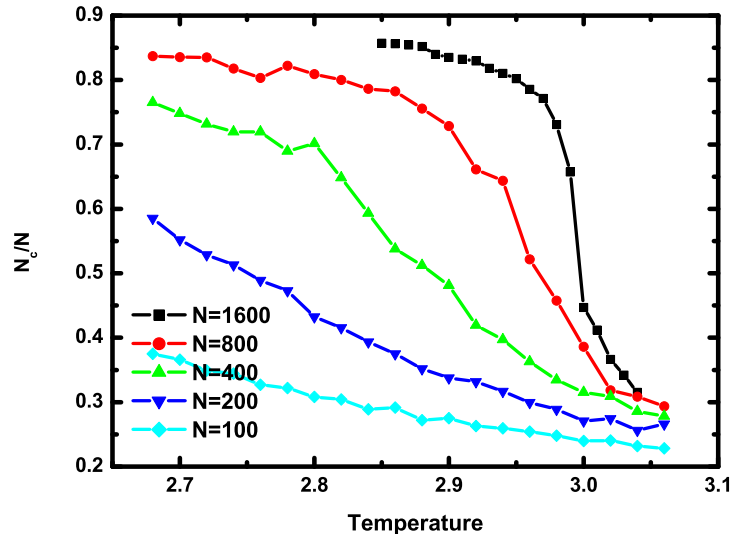


FIG. 9: (Color Online) The order parameter n_c as a function of temperature T for a semiflexible chain with $\epsilon_b = 5.0$ and different lengths N .

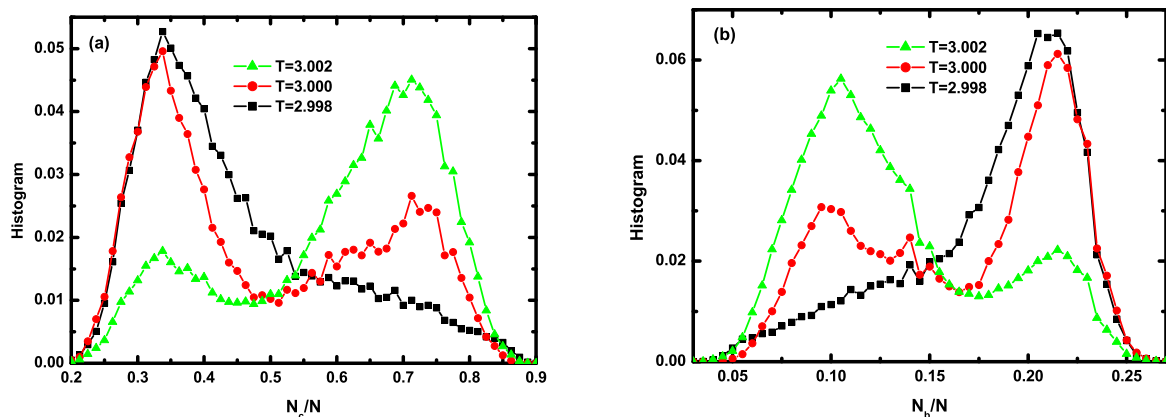


FIG. 10: (Color Online) Distribution of contact number N_c (a) and bending number N_b (b) for a semiflexible polymer with bending stiffness $\epsilon_b = 5.0$ and length $N = 1,600$. Different curves correspond to slightly different temperatures.

Fig. 10(a) and Fig. 10(b) report the distributions of the polymer's contacting number N_c and bending number N_b . When the temperature T is close to $T = 3.0$, there are two peaks in both probability distributions, indicating the system is bistable (both in terms of N_c and N_b) in this temperature range. The positions of these two peaks in the distribution of N_c and that of N_b remain almost fixed when the temperature changes, but their weights changes. As temperature increases, the system has higher probability to be in the coil phase. We can define the crystal-coil transition temperature as the temperature at which the system has equal probability to be in the crystal and the coil phase. This transition is between the crystal phase and the coil phase, because both the order parameters n_c and n_b will jump in the thermodynamic limit of $N \rightarrow \infty$ rather than just one of them.

We have performed the same analysis for other values of the bending stiffness ϵ_b . At zero external force, the complete phase-diagram of a 2D lattice polymer is shown in Fig. 11. When $\epsilon_b < \epsilon_b^* \approx 1.5$, the polymer has two structural phase-transitions as temperature changes, a first-order crystal-globule transition followed by a higher-temperature continuous globule-coil transition. When $\epsilon_b > \epsilon_b^*$, the polymer will transit directly from the crystal phase to the coil phase. In Ref. [22], it was predicted based on a partially directed 2D lattice model that, the collapse transition is

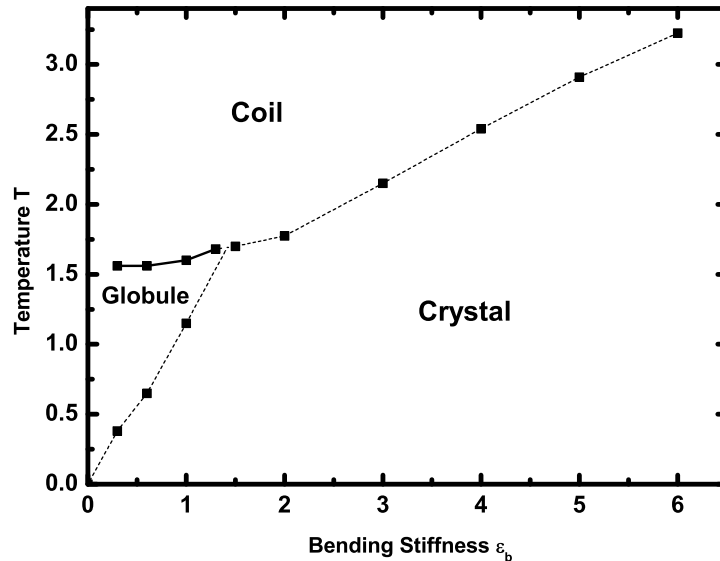


FIG. 11: The zero-force phase-diagram of the 2D lattice polymer. Square symbols are simulation results. The crystal-globule transition and the crystal-coil transition is first-order (as indicated by dashed boundary lines) in the thermodynamic limit, while the globule-coil transition is continuous (solid boundary line).

first-order as long as the bending stiffness is positive. This apparent contradiction between Ref. [22] and the present work is easy to understand. In the partially directed polymer model, the compact phase, since it is highly ordered, is not the disordered globule phase but rather the crystal phase. Because of the additional constraint of partial directness, the entropy of the compact phase is suppressed compared to that of the disordered globule phase. The simulation results of Fig. 11 also suggests that the crystal-coil transition temperature increases almost linearly with the bending stiffness ϵ_b , in consistence with the earlier work of Doniach and co-workers on 3D lattice polymers¹³.

V. FORCE-INDUCED PHASE-TRANSITIONS

With the zero-force phase-diagram Fig. 11 being obtained for a 2D lattice polymer, we now proceed to study its force-induced structural transitions. Initially the polymer is in a low temperature crystal or disordered globule phase. An external force along the x -direction is applied to the free end of the polymer, and the x -component of the polymer's extension, X_N , the contacting number N_c , the bending number N_b are recorded during the stretching.

A. The globule-coil transition

For a 2D lattice polymer with bending stiffness $\epsilon_b < 1.5$, we can choose an appropriate temperature value (say $T = 1.2$) such that, at zero external force, the polymer is in the disordered globular phase. At this temperature, when the external force f becomes sufficiently large, the globular shape of the polymer will be destroyed. The polymer will be in a highly extended coil configuration. As has been predicted by several earlier theoretical work^{22,25}, in the thermodynamic limit of $N \rightarrow \infty$, a globule-coil transition will take place at certain critical force $f_{cr}(T)$. In agreement with Ref. [25], we find this 2D force-induced globule-coil transition is a continuous transition.

The continuous nature of the force-induced globule-coil transition is checked by investigating the fluctuation of the elongation X_N . Figure 12 shows how the extension susceptibility χ_f of a flexible polymer system ($\epsilon_b = 0$) at $T = 1.2$ changes with force f . The extension susceptibility is defined by

$$\chi_f \equiv \frac{1}{N} \frac{\partial \langle X_N \rangle}{\partial f} = \beta [\langle X_N^2 \rangle - \langle X_N \rangle^2] / N . \quad (9)$$

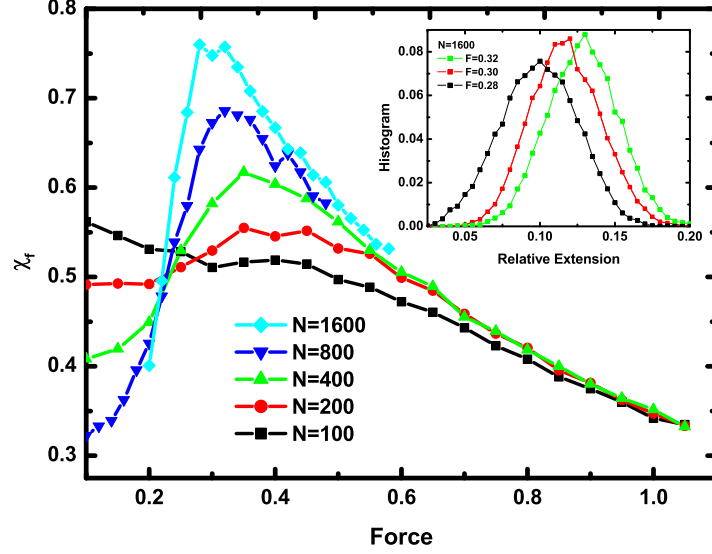


FIG. 12: (Color Online) The extension susceptibility χ_f as a function of external force f at $T = 1.2$ for a polymer with $\epsilon_b = 0$ and chain length N . Inset shows the distributions of normalized mean extension $\langle X_N \rangle / N$ for the polymer system with $N = 1,600$ near the globule-coil transition.

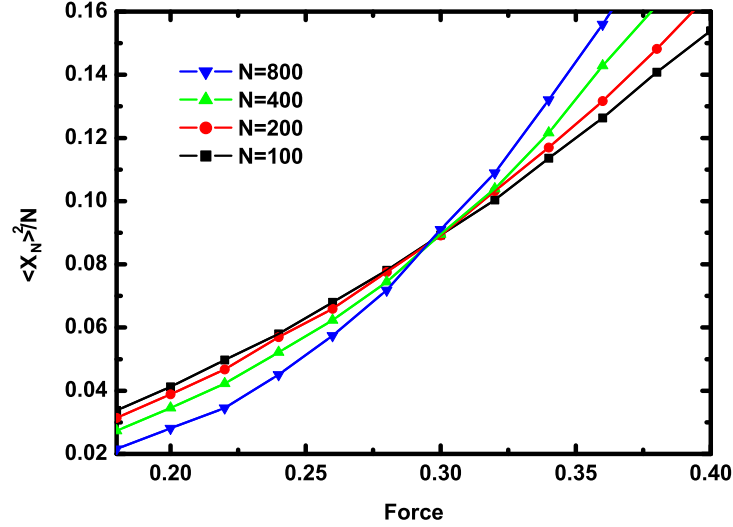


FIG. 13: (Color Online) The value of $\langle X_N \rangle^2 / N^{1.74}$ as a function of external force f for a flexible polymer ($\epsilon_b = 0$) of different lengths N . Different curves intersect at $f \approx 0.295$.

Figure 12 demonstrated that, as the chain length N increases, the peak of χ_f becomes more pronounced (eventually it will approach infinity). This behavior is very similar to the divergence of the specific heat $c(T)$ at the temperature-induced globule-coil transition (see Sec. IV). By finite-size scaling and extrapolating to the case of $N = \infty$ we obtain a transition force $f_{cr} \approx 0.3$ for the system (an more precise estimate of the transition is reported below). The inset of Fig. 12 shows the distribution of the extension of the system at different external forces. When the external force is close to the transition force f_{cr} , the extension distribution has only one peak which moves with force. This behavior further confirms the continuous nature of the structural transition.

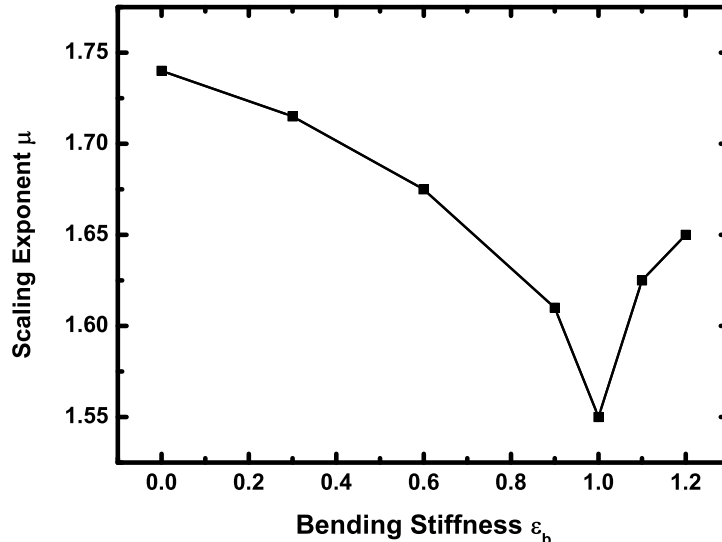


FIG. 14: The critical scaling exponent μ_{cr} at the globule-coil transition of Eq. (10) as a function of the bending stiffness ϵ_b at temperature $T = 1.2$.

Under an external force, we can write down the following effective scaling relation between the mean extension of the polymer and the chain length N :

$$\langle X_N \rangle^2 \sim N^\mu \quad (10)$$

with effective exponent μ . In the globule phase, the polymer is in an elliptic shape and μ in Eq. (10) is less than 2 but larger than 1. μ may increase with force f and reach a limiting value μ_{cr} at the globule-coil transition point. When f further increases and the polymer is in the coil phase, the extension of the polymer scales linearly with chain length N , i.e., $\mu = 2$. As in Sec. IV, we expect that, at the globule-coil transition point, the critical exponent μ_{cr} will be independent of chain length N . Then if $\langle X_N \rangle^2 / N^{\mu_{cr}}$ is plotted as a function of f , curves corresponding to different chain length N will intersect at the same point f_{cr} . Figure 13 demonstrates that this is indeed the case, and from this plot we estimate that $f_{cr} = 0.295$ and $\mu_{cr} = 1.74$ for a flexible polymer at $T = 1.2$. This value of f_{cr} is in agreement with Ref. [25], which predicted $f_{cr} \approx 0.30$. To further validate this method of determining the critical force, we have used it to determine the critical force for a flexible 2D partially directed polymer at $T = 0.59$ as studied in Ref. [22]. We obtained that the critical force $f_{cr} = 0.45$ (very close to the exactly known value 0.46) and $\mu_{cr} = 1.2$.

For $T = 1.2$ we have determined the critical exponent μ_{cr} for 2D lattice polymers with different bending stiffness ϵ_b . The critical exponent μ_{cr} is not a constant. It drops from the value of $\mu_{cr} = 1.74$ for $\epsilon_b = 0$ to $\mu_{cr} = 1.55$ for $\epsilon_b = 1.0$ (see Fig. 14). Intuitively this observation is natural to understand. At the force-induced globule-coil phase-transition point, the polymer takes the shape of an elongated ellipse²⁵. The bending stiffness ϵ_b affects the shape of this ellipse and therefore affects the critical exponent μ_{cr} . On the other hand, to derive an explicit expression for the relationship between μ and ϵ_b is a hard task. The critical exponent μ_{cr} may also depend on temperature.

The globule-coil transition force $f_{cr}(T)$ decreases with temperature almost linearly and vanishes at the θ -temperature T_θ , i.e., $f_{cr}(T) \sim (T_\theta - T)$ for $T < T_\theta$ (see Fig. 15). This linear relationship holds both for flexible and semiflexible chains.

B. The crystal-coil transition

At low temperature and zero force, a considerably stiff semiflexible polymer is in the crystal phase. We now investigate the force-induced crystal-coil transition by MC simulation. Since at $f = 0$, the temperature-induced crystal-coil transition is already a first-order transition, we expect the force-induced transition should also be first-order. This is confirmed by MC simulation results. Figure 16(a) shows the evolution of the total contacting number N_c of a polymer of length $N = 1,600$ and bending stiffness $\epsilon_b = 5.0$ at $T = 2.5$. At the three different force values,

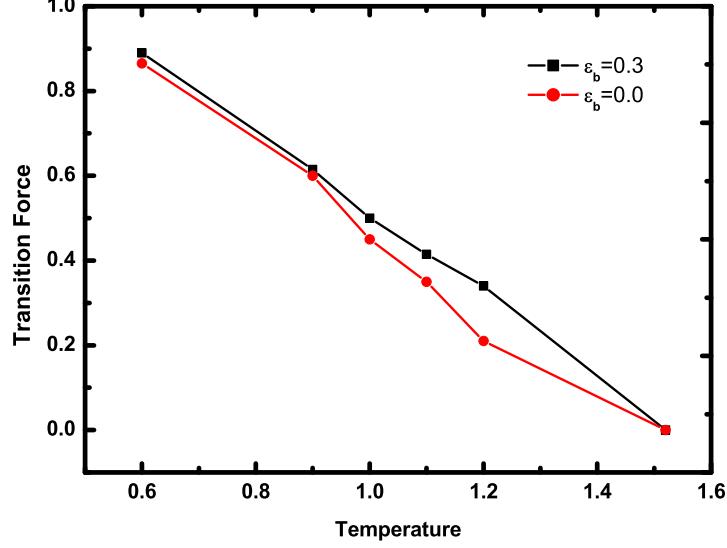


FIG. 15: The globule-coil transition force $f_{cr}(T)$ as a function of temperature T .

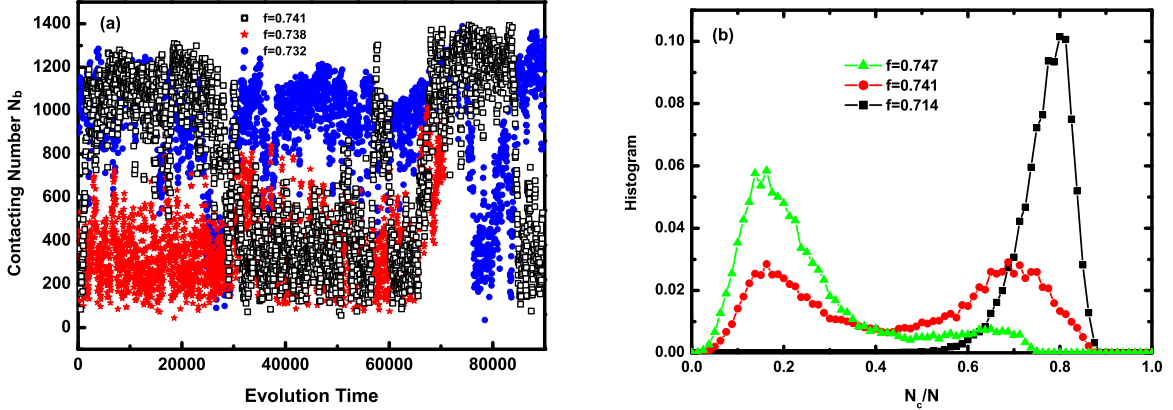


FIG. 16: (Color Online) The time evolution (a) and probability histogram (b) of the contacting number N_c of a polymer with $N = 1,600$ and $\epsilon_b = 5.0$. Different data sets correspond to different external force f , while the temperature is fixed at $T = 2.5$.

the contacting number jumps between the coiled shapes of $N_c \approx 300$ and the crystal shapes of $N_c \approx 1,000$. The histogram of the contacting number as shown in Fig 16(b) has two well-defined peaks for force $f \approx 0.74$. When f deviates remarkably from this value, however, one of the peaks in the contacting number histogram disappears, indicating the system is either in the crystal phase or in the coil phase.

Although the crystal-coil transition is a first-order phase-transition, if the chain length N is too small, the jump in the order parameter n_c or n_b can not be observed. This is because the correlation length at the crystal-coil transition may exceed the size of a small system. Figure 17 demonstrates that, for a polymer with bending stiffness $\epsilon_b = 5.0$ at temperature $T = 2.5$, only chains with length $N \geq 1,000$ will show clear signature of a discontinuous structural transition. When the chain length N is equal to 400 or 500, at the crystal-coil transition force (which corresponds to the maximum of the extension susceptibility χ_f), the two peaks of the distribution of n_c have the trend of merging into one peak. For these later small systems, the crystal-coil transition resembles a continuous phase-transition.

According to the phase-diagram Fig. 11, at fixed temperature T , there exists a threshold bending stiffness value $\epsilon_b^*(T)$ at which the force-induced collapse transition changes from being second-order to being first-order. To determine

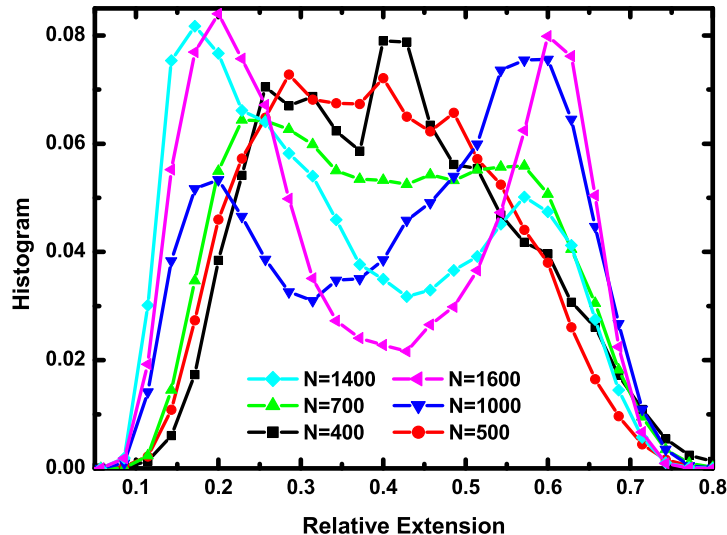


FIG. 17: (Color Online) Distribution of normalized mean extension $\langle X_N \rangle / N$ for a polymer with $\epsilon_b = 5.0$ at $T = 2.5$. The external force is set to the value at which the susceptibility χ_f reaches maximum, with $f = 0.68, 0.67, 0.70, 0.72, 0.73$ and 0.74 for $N = 400, 500, 700, 1,000, 1,400$ and $1,600$ respectively.

the value of ϵ_b^* precisely, however, is not easy. When the bending stiffness of the polymer is just slightly above ϵ_b^* , although an infinite chain will have a jump in the order parameters n_c and n_b at the collapse transition point, for a finite chain such jumps in n_c and n_b will be smeared out by large fluctuations of N_c and N_b at the transition point. For a polymer of length N less than or comparable to the correlation length of the system at the first-order collapse transition point, the elongation of the polymer may still follow the scaling rule Eq. (10), i.e., resembles a continuous structural transition. At $T = 1.2$, the critical exponent μ_{cr} (defined in the previous subsection) as a function of ϵ_b is shown in Fig. 14 for polymers of length up to $N = 1,000$. We find that μ_{cr} first decreases with ϵ_b ; but for $\epsilon_b > 1.0$ it increases with ϵ_b . We interpret this change of trend as follows: At a continuous collapse transition, the stiffer the chain is, the more compact it prefers and therefore the smaller the critical exponent μ is; on the other hand, at a discontinuous collapse transition, the stiffer the chain is, the more extended the average elongation of the polymer is and the larger the value of μ_{cr} is. Based on this argument, we estimate the value of ϵ_b^* as the point where the scaling exponent μ_{cr} reaches the minimal value.

VI. SUMMARY AND DISCUSSION

The qualitative properties of temperature- and force-induced collapse transitions of a 2D self-attractive semiflexible lattice polymer were investigated by Monte Carlo simulations. The system has three possible phases: the crystal phase, the disordered globular phase, and the random coil phase. The crystal-globule and the crystal-coil transitions are both first-order phase-transitions in the thermodynamic limit; while the globule-coil transition is a second-order phase transition. The disordered globular phase is absent for polymers of considerable stiffness. These simulation results are consistent with earlier theoretical¹³ and simulation^{14,29} studies on temperature-induced collapse transitions of 3D lattice polymers. They also confirm and extend the earlier simulation²⁵ and analytical^{22,30} studies on force-induced collapse transitions of 2D lattice polymers.

The simulation results also suggested that, at the continuous force-induced globule-coil transition, the extension of the polymer scales with polymer length according to $\langle X_N \rangle = a_0 N^{\frac{\mu_{cr}}{2}}$, with both a_0 and μ_{cr} being independent of chain length. Such a critical behavior is similar to the well-known critical scaling $R_g \propto a_1 N^{\nu_{cr}}$ at the temperature-induced globule-coil transition [see Eq. (6)], but it is yet to be confirmed by analytical calculations. According to the simulation results, the bending stiffness does not affect the critical exponent ν_{cr} . However, the scaling exponent μ_{cr} for the force-induced globule-coil transition changes with the bending stiffness ϵ_b (see Fig. 14). We suggest such a qualitative difference should be amenable to experimental verifications^{3,49}. A possible reason for this qualitative difference were also given in this paper.

For 2D polymers, we have shown that the temperature- and force-induced collapse transitions have the same order. This may not be the case for 3D polymers. For 3D flexible polymers, the force-induced globule-coil transition is a first-order phase-transition²⁵; the order of the temperature-induced collapse transition, on the other hand, is usually regarded as second-order in many references (but Binder and co-authors²³ argued that it is actually also a first-order phase-transition).

Acknowledgment

We are grateful to Luru Dai and Zhihui Wang for their helps on simulation techniques and programming. The computer simulation was performed at the PC clusters of the State Key Laboratory of Scientific and Engineering Computing, Beijing.

-
- ¹ J. des Cloizeaux and G. Jannink, *Polymers in Solution: Their Modelling and Structure* (Clarendon Press, Oxford, 1990).
² P.-G. de Gennes, *Scaling Concepts in Polymer Physics* (Cornell Univ. Press, New York, 1979).
³ B. Maier and J. O. Rädler, *Phys. Rev. Lett.* **82**, 1911 (1999).
⁴ P. J. Flory, *Principles of Polymer Chemistry* (Cornell University, Ithaca, 1967).
⁵ C. Vanderzande, *Lattice Models of Polymers* (Cambridge University Press, Cambridge, 1998).
⁶ B. Nienhuis, *Phys. Rev. Lett.* **49**, 1062 (1982).
⁷ B. Duplantier and H. Saleur, *Phys. Rev. Lett.* **59**, 539 (1987).
⁸ C. Bustamante, Z. Bryant, and S. B. Smith, *Nature* **421**, 423 (2003).
⁹ R. Zwanzig and J. I. Lauritzen, JR., *J. Chem. Phys.* **48**, 3351 (1968).
¹⁰ J. I. Lauritzen, JR. and R. Zwanzig, *J. Chem. Phys.* **52**, 3470 (1970).
¹¹ A. R. Massih and M. A. Moore, *J. Phys. A* **8**, 237 (1975).
¹² A. L. Owczarek and T. Prellberg, *Physica (Amsterdam)* **205A**, 203 (1994).
¹³ S. Doniach, T. Garel, and H. Orland, *J. Chem. Phys.* **105**, 1601 (1996).
¹⁴ J. P. K. Doye, R. P. Sear, and D. Frenkel, *J. Chem. Phys.* **108**, 2134 (1998).
¹⁵ A. Kloczkowski and R. L. Jernigan, *J. Chem. Phys.* **109**, 5134 (1998).
¹⁶ A. L. Owczarek and T. Prellberg, *Europhys. Lett.* **51**, 602 (2000).
¹⁷ C. Nowak, V. G. Rostiashvili, and T. A. Vilgis, *Euro. Phys. Lett.* **74**, 76 (2006).
¹⁸ S. Kumar and D. Giri, *Phys. Rev. Lett* **98**, 048101 (2007).
¹⁹ A. Y. Grosberg and A. R. Khokhlov, *Statistical Physics of Macromolecules* (AIP Press, New York, 1994).
²⁰ D. Marenduzzo, A. Maritan, A. Rosa, and F. Seno, *Phys. Rev. Lett.* **90**, 088301 (2003).
²¹ A. Rosa, D. Marenduzzo, and S. Kumar, *Europhys. Lett.* **75**, 818 (2006).
²² H. Zhou, J. Zhou, Z.-C. Ou-Yang, and S. Kumar, *Phys. Rev. Lett* **97**, 158302 (2006).
²³ R. Rampf, W. Paul, and K. Binder, *Europhys. Lett.* **70**, 628 (2005).
²⁴ K. Binder, J. Baschnagel, M. Muller, W. Paul, and F. Rampf, *Macromol. Symp.* **237**, 128 (2006).
²⁵ P. Grassberger and J. Hsu, *Phys. Rev. E.* **65**, 031807 (2002).
²⁶ P.-Y. Lai, *Chinese J. Phys.* **36**, 494 (1998).
²⁷ M. Wittkop, S. Kreitmeier, and D. Goritz, *J. Chem. Phys.* **104**, 3373 (1995).
²⁸ D. F. Parsons and D. R. M. Williams, *J. Chem. Phys.* **124**, 221103 (2006).
²⁹ U. Bastolla and P. Grassberger, *J. Stat. Phys.* **89**, 1061 (1997).
³⁰ D. Marenduzzo, A. Maritan, A. Rosa, and F. Seno, *Eur. Phys. J. E.* **15**, 83 (2004).
³¹ M. N. Rosenbluth and A. W. Rosenbluth, *J. Chem. Phys.* **23**, 356 (1995).
³² P. Grassberger, *Phys. Rev. E.* **56**, 3682 (1997).
³³ L. Dai, F. Liu, and Z.-C. Ou-Yang, *J. Chem. Phys.* **119**, 8124 (2003).
³⁴ L. Huang, X. He, Y. Wang, H. Chen, and H. Liang, *J. Chem. Phys.* **119**, 8124 (2003).
³⁵ K. Huang, *Biophys. Rev. Lett.* **2**, 139 (2007).
³⁶ Y.-P. Luo, M.-C. Huang, J.-W. Wu, T.-M. Liaw, and S. C. Lin, *J. Chem. Phys.* **126**, 134907 (2007).
³⁷ M. E. J. Newman and G. T. Barkema, *Monte Carlo Methods in Statistical Physics* (Oxford University Press, New York, 1999).
³⁸ I. M. Lifshitz, A. Y. Grosberg, and A. R. Khokhlov, *Rev. Mod. Phys* **50**, 683 (1978).
³⁹ P.-G. de Gennes, *J. Phys. Lett* **36**, L55 (1975).
⁴⁰ P.-G. de Gennes, *J. Phys. Lett* **39**, L299 (1975).
⁴¹ J. W. Halley, *J. Chem. Phys.* **88**, 5181 (1988).
⁴² H. Meirovitch and H. A. Lim, *J. Chem. Phys.* **91**, 2544 (1989).
⁴³ H. Meirovitch and H. A. Lim, *J. Chem. Phys.* **92**, 5144 (1990).
⁴⁴ A. M. Torres, A. Rubio, J. J. Freire, M. Bishop, and J. H. R. Clarke, *J. Chem. Phys* **100**, 7754 (1994).
⁴⁵ A. M. Rubio, J. J. Freire, M. Bishop, and J. H. R. Clarke, *Macromolecules* **28**, 2240 (1995).

- ⁴⁶ F. Seno and A. L. Stella, *J. Physique* **49**, 739 (1988).
- ⁴⁷ R. Vrak, A. L. owczarek, and t. Prellberg, *J. Phys. A: Math. Gen* **26**, 4565 (1993).
- ⁴⁸ Y. A. Kuznetsov, E. G. Timoshenko, and K. A. Dawson, *J. Chem. Phys.* **104**, 336 (1996).
- ⁴⁹ P.-K. Lin, C.-C. Fu, Y.-L. Chen, Y.-R. Chen, P.-K. Wei, C. H. Kuan, and W. s. Fann, *Phys. Rev. E* **76**, 011806 (2007).